

Potentials of Mean Force between Ionizable Amino Acid Side Chains in Water

Artém Masunov and Themis Lazaridis*

Contribution from the City College of the City University of New York, Convent Ave. at 138 St.,
New York, New York 10031

Received January 3, 2002; E-mail: themis@sci.cuny.edu.

Abstract: Potentials of mean force (PMF) between all possible ionizable amino acid side chain pairs in various protonation states were calculated using explicit solvent molecular dynamics simulations with umbrella sampling and the weighted histogram analysis method. The side chains were constrained in various orientations inside a spherical cluster of 200 water molecules. Beglov and Roux's Spherical Solvent Boundary Potential was used to account for the solvent outside this sphere. This approach was first validated by calculating PMFs between monatomic ions (K^+ , Na^+ , Cl^-) and comparing them to results from the literature and results obtained using Ewald summation. The strongest interaction (-4.5 kcal/mol) was found for the coaxial $Arg^+...Glu^-$ pair. Many like-charged side chains display a remarkable lack of repulsion, and occasionally a weak attraction. The PMFs are compared to effective energy curves obtained with common implicit solvation models, namely Generalized Born (GB), EEF1, and uniform dielectric of 80. Overall, the EEF1 curves are too attractive, whereas the GB curves in most cases match the minima of the PMF curves quite well. The uniform dielectric model, despite some fortuitous successes, is grossly inadequate.

Introduction

Salt bridges are thought to play an important role in protein stability and protein-protein interactions. Perutz attributed the enhanced stability of a thermophilic ferredoxin compared to a mesophilic analogue to the increased number of surface salt bridges.¹ However, the free energy contribution of salt bridges remains controversial. Experimental measurements in peptide and protein models yield a net stabilization ranging from -0.5 to -5 kcal/mol.²⁻⁸ Other experiments report partly buried salt bridges to be destabilizing by 2 to 4 kcal/mol.^{9,10} Apparently, the net effect of a salt bridge is a delicate balance between the high cost of desolvating the ions and the interionic attraction. Even if salt bridges are destabilizing, they provide specificity, i.e., they limit the number of low free energy conformations and thus can be used in the rational design of proteins.^{11,12} In addition, they may increase the thermostability of proteins because the desolvation penalty for the ionic side chains decreases at high temperature more than that for hydrophobic

ones.¹³ Salt bridges also affect the kinetics of protein folding and protein-protein association.¹⁴

One fundamental measure of the interaction between solutes in solution is the potential of mean force (PMF), i.e., the free energy as a function of the configuration of the solutes. Theoretical calculation of the PMF is not a trivial task. Especially crucial in the case of charged species is the treatment of long-range interactions. Several groups have calculated the PMF between monatomic or small molecular ions in water. Friedman and Mezei¹⁵ used adaptive umbrella sampling with Monte Carlo (MC) simulations to calculate the $Na^+...Cl^-$ PMF. They concluded that both the number and the depth of the minima vary significantly when different boundary conditions are used. In their molecular dynamics (MD) free energy calculations, Rozanska and Chipot¹⁶ studied the guanidinium-acetate interaction in water using 3 different boundary conditions: Ewald summation (EW), generalized reaction field correction, and conventional spherical truncation. EW gave a physically reasonable result with a relatively flat PMF in the 8 to 11 Å range and a contact minimum (CM) more stable than the solvent-separated minimum (SSM). The conventional cutoff yielded a PMF that was about 6 kcal/mol lower than the EW PMF at 9 Å, and kept decreasing beyond 10 Å. The use of a reaction field correction brought the PMF closer to that from EW. Cutoff artifacts were also noticed in a study of the PMF between ferrous and ferric ions.¹⁷ With Ewald summation the PMF was monotonically repulsive. A decreasing $Na^+...Cl^-$ PMF

- (1) Perutz, M. F. *Science* **1978**, *201*, 1187.
- (2) Lyu, P. C.; Gans, P. J.; Kallenbach, N. R. *J. Mol. Biol.* **1992**, *223*, 343.
- (3) Smith, J. S.; Scholtz, J. M. *Biochemistry* **1998**, *37*, 33.
- (4) Anderson, D. E.; Becktel, W. J.; Dahlquist, F. W. *Biochemistry* **1990**, *29*, 2403.
- (5) de Prat Gay, G.; Johnson, C. M.; Fersht, A. R. *Protein Engin.* **1994**, *7*, 103.
- (6) Marqusee, S.; Sauer, R. T. *Protein Sci.* **1994**, *3*, 2217.
- (7) Tissot, A. C.; Vuillemeier, S.; Fersht, A. R. *Biochemistry* **1996**, *35*, 6786.
- (8) Spek, E. J.; Bui, A. H.; Lu, M.; Kallenbach, N. R. *Protein Sci.* **1998**, *7*, 2431.
- (9) Schneider, J. P.; Lear, J. D.; DeGrado, W. F. *J. Am. Chem. Soc.* **1997**, *119*, 5742.
- (10) Waldburger, C. D.; Schildbach, J. F.; Sauer, R. T. *Nature Struct. Biol.* **1995**, *2*, 122.
- (11) Sindelar, C. V.; Hendsch, Z. S.; Tidor, B. *Protein Sci.* **1998**, *7*, 1898.
- (12) Spector, S.; Wang, M.; Carp, S. A.; Robblee, J.; Hendsch, Z. S.; Fairman, R.; Tidor, B.; Raleigh, D. P. *Biochemistry* **2000**, *39*, 872.

- (13) Elcock, A. H. *J. Mol. Biol.* **1998**, *284*, 489.
- (14) Waldburger, C. D.; Jonsson, T.; Sauer, R. T. *Proc. Natl. Acad. Sci. U.S.A.* **1996**, *93*, 2629.
- (15) Friedman, R. A.; Mezei, M. *J. Chem. Phys.* **1995**, *102*, 419.
- (16) Rozanska, X.; Chipot, C. *J. Chem. Phys.* **2000**, *112*, 9691.
- (17) Bader, J. S.; Chandler, D. *J. Phys. Chem.* **1992**, *96*, 6423.

at 6–7 Å was also found in MC simulations with periodic/minimum image boundary conditions.¹⁸ Particle Mesh EW in conjunction with the thermodynamic integration method on the aqueous Na⁺...Cl⁻ system yielded a physically reasonable flat PMF in the range 6 to 9 Å and two stable minima (CM significantly more stable than SSM).¹⁹

The PMFs for like charged ions are somewhat controversial and are sensitive to the short-range behavior of the potentials and the boundary conditions. Pettitt and Rossky obtained a minimum of $w = -0.85$ kcal/mol for the Cl⁻...Cl⁻ ion pair in their RISM/HCN study.²⁰ This result was reproduced by MD simulations.^{21,22} The existence of Cl⁻...Cl⁻ as a stable aqueous species has been explained by the stabilizing effect of the hydrogen-bonded bridges Cl⁻(HOH)_{*n*}Cl⁻, which can overcome the Coulombic repulsion.^{22,23} However, Hummer et al. found no Cl⁻...Cl⁻ pairing in their simulations^{24,25} and Yu et al.²⁶ obtained only one local minimum of $w = 0.3$ kcal/mol at $r = 4.0$ Å for the Cl⁻...Cl⁻ ion pair, when they used a harder repulsive Lennard–Jones potential for this interaction within the DRISM/HNC theory. The crucial role of the potential used was confirmed by Dang and Pettitt.²⁷ Guàrdia et al.²⁸ also found an unstable local minimum for Cl⁻...Cl⁻ and pointed out the unphysical consequences of a deep minimum for two Cl⁻ ions. Zhong and Friedman²⁹ also found that using the attractive PMF of Pettitt and Rossky led to disagreement of the calculated diffusion coefficient of Cl⁻...Cl⁻ ion pairs with experiment. Kovalenko and Hirata^{30,31} used elaborate 3D-RISM treatments and also found unstable local minima on PMFs for Cl⁻...Cl⁻ and Na⁺...Na⁺. Buckner and Jorgensen³² used MC simulation and the TIP4P water model and found no minimum on the PMF between tetramethylammonium ions, whereas the Cl⁻...Cl⁻ ion pair had a minimum of $w = -4.5$ kcal/mol at $r = 5$ Å. Using similar methodology, guanidinium ions were found to have a stable minimum ranging from -10 kcal/mol (with the TIP4P water model)³³ to -2.7 kcal/mol (with the polarizable SPC water model).³⁴

Application of implicit solvation models allows the study of larger systems, including proteins. Solutions of the linearized Poisson–Boltzmann (PB) equation³⁵ gave insights into electrostatic effects in rigid conformations of proteins.^{36,37} The more computationally efficient Generalized Born (GB) model³⁸ allowed Gilson and co-workers³⁹ to explore the entire conformational ensemble of salt bridges in isolated ion pairs and in

proteins. For the guanidinium–hydrophosphate ion pair they found the effective energy of bringing the ions together at fixed orientation to be -3.8 kcal/mol. The binding free energy of the unconstrained ion pair in solution, which involves thermal averaging, was found to be -1 kcal/mol (about twice as large as the experimental value), and the guanidinium–hydrophosphate contribution to the binding affinity of a host–guest complex was found to be -2.5 kcal/mol (almost exactly matching the experimental estimate). Somewhat weaker stabilizing effects of the salt bridge were found for the oppositely charged side chains at (*i*, *i* + 4) positions of helical peptides. These results show that the salt bridge becomes stronger when partially constrained by the covalent environment and that the effective energy gives an upper estimate for the free energy of salt bridge formation.

Simple implicit solvation models that neglect packing effects, such as uniform dielectric screening or GB, predict only one minimum on the effective energy curve. However, empirically parametrized models based on solvent accessible surface area and a penalty for excluded volume were shown to reproduce the PMF obtained in explicit simulations.^{40–42} PB models can also predict a double-minimum PMF for oppositely charged (but not like-charged) ion pairs if the dielectric boundary is defined in a certain way⁴³ but quantitative agreement can only be achieved with careful parametrization.⁴⁴ A parametrization for the solvation free energy of molecular ions based on PB plus a solvent accessible surface area component was proposed by Honig and co-workers⁴⁵ and extended to high temperatures by Elcock and McCammon.⁴⁶ Detailed description of the boundary between low-dielectric molecular interior and high-dielectric solvent allowed the reproduction of both CM and SSM for ethylammonium-acetate.¹³ Ab initio calculations on small organic ions with the polarizable continuum model or variants thereof have also been reported.^{47,48}

Our long-term interest is in the development of effective energy functions for biological macromolecules.⁴⁹ In these energy functions electrostatic interactions, and especially charge–charge interactions, make the largest contributions. Therefore, the proper description of such interactions is critical for the success of the function. One simple test is to compare the results of an effective energy function to PMFs obtained by explicit solvent simulations. To that end, we report here the PMF between ionizable amino acid side chains (Arg, Lys, His, Glu/Asp) in water. The results were obtained using the Spherical Solvent Boundary Potential (SSBP).⁵⁰ Because this potential has not yet been used for PMF calculations, it is first validated by calculating the PMFs of monatomic ions (K⁺, Na⁺, Cl⁻) and comparing them to previous results and to results obtained using Ewald summation. The calculated PMFs are compared to effective energy curves obtained with three common models implemented in CHARMM: Generalized Born,⁵¹ EEF1,⁵² and uniform dielectric of 80 (primitive electrolyte model).

- (18) Resat, H.; Mezei, M.; McCammon, J. A. *J. Phys. Chem.* **1996**, *100*, 1426.
 (19) Martorana, V.; Fata, L. L.; Bulone, D.; San Biagio, P. L. *Chem. Phys. Lett.* **2000**, *329*, 221.
 (20) Pettitt, B. M.; Rossky, P. J. *J. Chem. Phys.* **1986**, *84*, 5836.
 (21) Dang, L. X.; Pettitt, B. M. *J. Am. Chem. Soc.* **1987**, *109*, 5531.
 (22) Dang, L. X.; Pettitt, B. M. *J. Phys. Chem.* **1990**, *94*, 4303.
 (23) Friedman, G. L. *Faraday Discuss. Chem. Soc.* **1988**, *85*, 1.
 (24) Hummer, G.; Soumpasis, D. M.; Neumann, M. *Mol. Phys.* **1992**, *77*, 769.
 (25) Hummer, G.; Soumpasis, D. M.; Neumann, M. *Mol. Phys.* **1994**, *81*, 1155.
 (26) Yu, H.-A.; Roux, B.; Karplus, M. *J. Chem. Phys.* **1990**, *92*, 5020.
 (27) Dang, L. X.; Pettitt, B. M.; Rossky, P. J. *J. Chem. Phys.* **1992**, *96*, 4046.
 (28) Guardia, E.; Rey, R.; Padro, J. A. *J. Chem. Phys.* **1991**, *95*, 2823.
 (29) Zhong, E. C.; Friedman, H. L. *J. Phys. Chem.* **1988**, *92*, 1685.
 (30) Kovalenko, A.; Hirata, F. *J. Chem. Phys.* **2000**, *112*, 10 391.
 (31) Kovalenko, A.; Hirata, F. *J. Chem. Phys.* **2000**, *112*, 10 403.
 (32) Buckner, J. K.; Jorgensen, W. L. *J. Am. Chem. Soc.* **1989**, *111*, 2507.
 (33) Boudon, E.; Wipff, G.; Maigret, B. *J. Phys. Chem.* **1990**, *94*, 6056.
 (34) Soetens, J.-C.; Millot, C.; Chipot, C.; Jansen, G.; Angyan, J. G.; Maigret, B. *J. Phys. Chem. B* **1997**, *101*, 10 910.
 (35) Honig, B.; Sharp, K.; Yang, A.-S. *J. Phys. Chem.* **1993**, *97*, 1101.
 (36) Hendsch, Z. S.; Tidor, B. *Prot. Sci.* **1994**, *3*, 211.
 (37) Rashin, A. A. *Proteins* **1992**, *13*, 120.
 (38) Still, W. C.; Tempczyk, A.; Hawley, R. C.; Hendrickson, T. *J. Am. Chem. Soc.* **1990**, *112*, 6127.
 (39) Luo, R.; David, L.; Hung, H.; Devaney, J.; Gilson, M. K. *J. Phys. Chem. B* **1999**, *103*, 727.

- (40) Fukunishi, Y.; Suzuki, M. *J. Phys. Chem.* **1996**, *100*, 5634.
 (41) Fukunishi, Y.; Suzuki, M. *J. Comput. Chem.* **1997**, *18*, 1656.
 (42) Shimizu, S.; Chan, H.-S. *Proteins* **2002**, *48*, 15.
 (43) Rashin, A. A. *J. Phys. Chem.* **1989**, *93*, 4664.
 (44) Pratt, L. R.; Hummer, G.; Garcia, A. E. *Biophys. Chem.* **1994**, *51*, 147.
 (45) Sitkoff, D.; Sharp, K. A.; Honig, B. *J. Phys. Chem.* **1994**, *98*, 1978.
 (46) Elcock, A. H.; McCammon, J. A. *J. Phys. Chem.* **1997**, *101*, 9624.
 (47) No, K. T.; Nam, K.-Y.; Scheraga, H. A. *J. Am. Chem. Soc.* **1997**, *119*, 12 917.
 (48) Cho, K.-H.; No, K. T.; Scheraga, H. A. *J. Phys. Chem. A* **2000**, *104*, 6505.
 (49) Lazaridis, T.; Karplus, M. *Curr. Opin. Struct. Biol.* **2000**, *10*, 139.
 (50) Beglov, D.; Roux, B. *J. Chem. Phys.* **1994**, *100*, 9050.

Methods

All calculations were performed using the CHARMM program (version c28b0 or c28a4) with the polar hydrogen CHARMM 19 force field^{53,54} for the side chains and the CHARMM 27 force field for K^+ ($\sigma = 3.143 \text{ \AA}$, $\epsilon = 0.087 \text{ kcal/mol}$), Na^+ ($\sigma = 2.43 \text{ \AA}$, $\epsilon = 0.047 \text{ kcal/mol}$), and Cl^- ($\sigma = 4.045 \text{ \AA}$, $\epsilon = 0.150 \text{ kcal/mol}$). The TIP3P model was used for water, as this model's macroscopic dielectric permittivity was estimated to be $\epsilon = 82$, close to the experimental value.⁵⁵

For polyatomic ions the PMF is a function of distance and the relative orientation of the ions. The ideal would be to calculate a multidimensional PMF. Because this is computationally prohibitive, we sampled one or more well-defined orientations and used the distance between the nearest heavy atoms as a reaction coordinate r . In all cases the ions were constrained to move on a straight line. The PMFs were calculated using Umbrella Sampling,⁵⁶ as implemented in CHARMM.⁵⁷ In this method the system is constrained to a narrow range of the reaction coordinate by application of a quadratic biasing potential $V(r) = k_{umb}(r - r_0)^2$. The frequency distribution $P_i(r)$ for each window i is then converted into free energy using the formula

$$W_i(r) = -k_B T \ln(P_i(r)) - V_i(r) + C_i$$

where k_B is Boltzmann's constant, and C_i is an undetermined constant.

To cover the range of interest (3 to 9 \AA) 7 windows were typically used (centered at 3, 4, 5, 6, 7, 8, and 9 \AA), and a MD run of 200 ps was performed for each window. This allows us to obtain data up to a distance of about 10.5 \AA . Initially, umbrella potentials with $k_{umb} = 1 \text{ kcal/\AA}^2$ were applied in all windows. In some cases, this force constant was found insufficient to sample near the top of high energy barriers and additional simulations were performed using $k_{umb} = 4$ or 7 kcal/\AA^2 centered at the barrier. The results were postprocessed using the weighted histogram analysis method (WHAM).⁵⁸ In this method histograms $P_i(r)$ obtained in each window are combined and the factors C_i are iteratively fit to yield an optimal solution that satisfies the continuity constraint. The resulting PMF was shifted vertically to match the values predicted for dielectric continuum with $\epsilon = 80$ at the longest possible distance (typically 9.5 to 10.5 \AA).

All pairs of ionizable amino acid side chains (up to C^β) were studied. The side chains were constrained to remain in specific orientations. A spherical water cluster of 200 molecules (radius 11 \AA) was built centered at the midpoint of the constrained ion pair. A cutoff of 20 \AA was used for the nonbonded interactions, including essentially all interactions in the cluster. The water molecules were subject to the Spherical Solvent Boundary Potential, parametrized to reproduce the electrostatic and van der Waals effect of bulk water at constant pressure.⁵⁰ All calculations were performed with the center of mass of the two ions harmonically constrained to the center of the sphere. This is consistent with the formal definition of SSBP which implies that the solute is kept at the center of the explicit solvent region (practically, the ions would absorb to the boundary if they were completely free to move). These constraints were implemented using the GEO command in CHARMM.

To check the dependence of the results on the size of the sphere, we also performed a calculation of the $Na^+ \dots Cl^-$ PMF in a larger sphere with 1653 water molecules (radius $\sim 23 \text{ \AA}$). Initially we employed the same nonbonded cutoff as in the small sphere and obtained a PMF continuously decreasing at long distances, as observed previously.¹⁶ This is presumably due to the fact that truncation allows

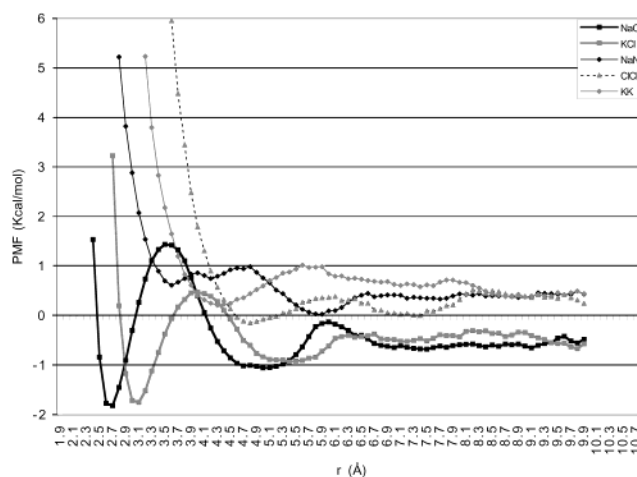


Figure 1. PMFs between the K^+ , Na^+ , and Cl^- ions in a 200 water cluster with the SSBP boundary condition.

some water molecules polarized by one ion to avoid unfavorable interactions with the other ion. The results reported here were performed using “extended electrostatics”, where interactions beyond the cutoff are treated using a multipole moment approximation.⁵⁹ We also performed a calculation of the same PMF in a cubic box of 31.1 \AA (995 water molecules) using Ewald summation and the same real space cutoff as above. The computational cost of the Ewald or large sphere calculations was about 30 times that of the small sphere calculations.

Results and Discussion

The PMFs between the ions K^+ , Na^+ , and Cl^- obtained using SSBP in a 200 water sphere are shown in Figure 1. All PMFs are well behaved at long distances, i.e., they are quite flat from 6.5 to 10 \AA . The unlike charged pairs $Na^+ \dots Cl^-$ and $K^+ \dots Cl^-$ exhibit a well-defined contact minimum and a less structured solvent separated minimum. The like charged pairs $Na^+ \dots Na^+$, $Cl^- \dots Cl^-$, and $K^+ \dots K^+$ exhibit shallow contact minima with slightly positive energies. These PMFs are qualitatively similar to those previously obtained in the literature. Quantitative comparison is difficult since those studies employ different potentials for the ions and/or water. The largest amount of data are available for the NaCl system. Our $Na^+ \dots Cl^-$ PMF is similar to that reported by Smith and Dang⁶⁰ and Lyubartsev and Laaksonen at 0.5 M concentration,⁶¹ except for a deeper CM and a higher barrier between CM and SSM in the present study. Martorana et al.¹⁹ found an even deeper CM and a more shallow SSM. Degreve and da Silva⁶² also found a more shallow SSM and a CM less deep than that of the present study. The $Na^+ \dots Na^+$ PMF obtained here is slightly more repulsive and less structured than that calculated previously.^{28,61,62} Our $Cl^- \dots Cl^-$ PMF is slightly less repulsive than that of Lyubartsev and Laaksonen at 0.5 M concentration⁶¹ and Guardia et al.²⁸ and slightly less attractive than that of Degreve and da Silva.⁶²

Figure 2 compares the PMFs obtained for $Na^+ \dots Cl^-$ in the 200 water sphere with SSBP, a 1653 water sphere with SSBP, and a 31.1 \AA cubic box using Ewald summation. The results are quite similar. The CM with Ewald summation is the deepest and that of the small sphere the most shallow. There is also some difference between the SSBP and Ewald results around 6

(51) Dominy, B. N.; Brooks, C. L., III *J. Phys. Chem. B* **1999**, *103*, 3765.

(52) Lazaridis, T.; Karplus, M. *Proteins* **1999**, *35*, 133.

(53) Brooks, B. R.; Brucoleri, R. E.; Olafson, B. D.; States, D. J.; Swaminathan, S.; Karplus, M. *J. Comput. Chem.* **1983**, *4*, 187.

(54) Neria, E.; Fischer, S.; Karplus, M. *J. Chem. Phys.* **1996**, *105*, 1902.

(55) Kusalik, P. G.; Svishchev, I. M. *Science* **1994**, *265*, 1219.

(56) Torrie, G. M.; Valleau, J. P. *J. Comput. Phys.* **1977**, *23*, 187.

(57) Kottalam, J.; Case, D. A. *J. Am. Chem. Soc.* **1988**, *110*, 7690.

(58) Kumar, S.; Bouzida, D.; Swendsen, R. H.; Kollman, P. A.; Rosenberg, J. M. *J. Comput. Chem.* **1992**, *13*, 1011.

(59) Stote, R. H.; States, D. J.; Karplus, M. *J. Chim. Phys.* **1991**, *88*, 2419.

(60) Smith, D. E.; Dang, L. X. *J. Chem. Phys.* **1994**, *100*, 3757.

(61) Lyubartsev, A. P.; Laaksonen, A. *Phys. Rev. A* **1997**, *55*, 5689.

(62) Degreve, L.; da Silva, F. L. B. *J. Chem. Phys.* **1999**, *110*, 3070.

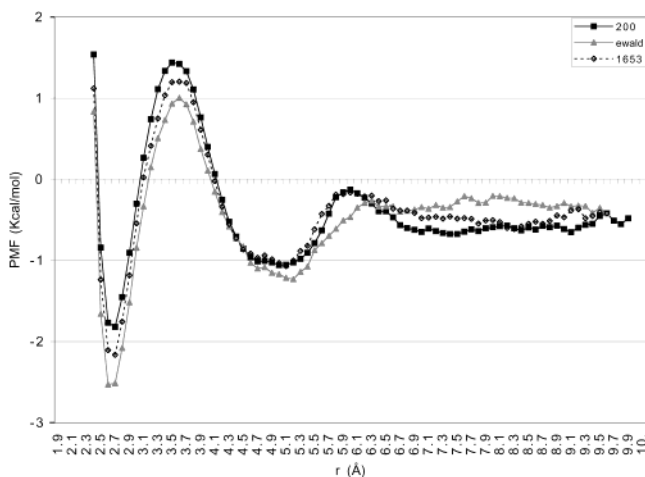


Figure 2. PMFs for $\text{Na}^+\dots\text{Cl}^-$ using Ewald summation, SSBP in a 200 water sphere, and SSBP in a 1653 water sphere.

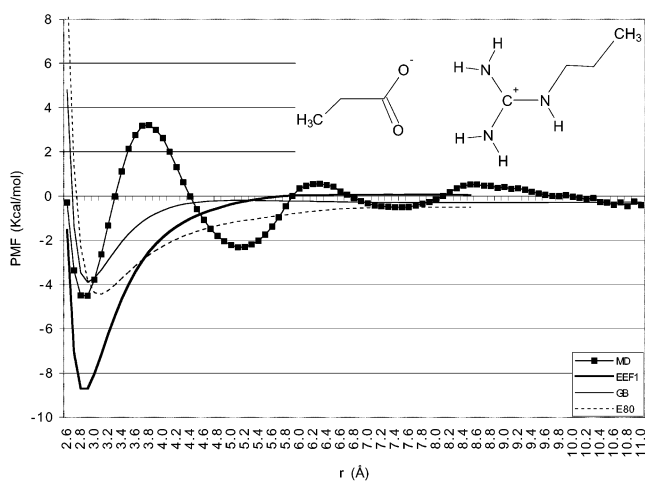


Figure 3. PMF and effective energy curves for the $\text{Arg}^+\dots\text{Glu}^-$ ion pair. r is the distance between the OE atoms of Glu and the NH atoms of Arg.

Å. Clearly, these differences could be partly due to statistical uncertainty (sampling error) and should be analyzed in more detail by performing longer simulations and varying the parameters of the simulations. For the purposes of this work, however, the quality of the small sphere results appears satisfactory. All the remaining calculations were performed using the 200 water sphere.

The PMFs between molecular ions that correspond to amino acid side chains are reported on Figures 3–17 (lines with markers). Most structured is the PMF of unlike-charged ions $\text{Arg}^+\dots\text{Glu}^-$ for a coplanar, double H-bond forming approach (Figure 3). In this calculation the guanidinium and acetate moieties are constrained to be on the same plane and the atoms CZ, NE of Arg and CD, CG of Glu are constrained on a line. The CM and SSM of $w = -4.5$ kcal/mol at $r = 2.8$ Å and -2.3 kcal/mol at $r = 5.2$ Å, respectively, as well as the barrier of 7.7 kcal/mol for escape from CM are in qualitative agreement with results obtained using Ewald summation and the AMBER force field¹⁶ for guanidinium–acetate (our CM is deeper). The GB and primitive models closely approximate the depth of the CM, whereas EEF1 overestimates it significantly.

Another pair of unlike charged ions ($\text{Lys}^+\dots\text{Glu}^-$) in two different orientations is reported on Figure 4a,4b. In the first (head to head) orientation the NZ, CE atoms of Lys and CD,

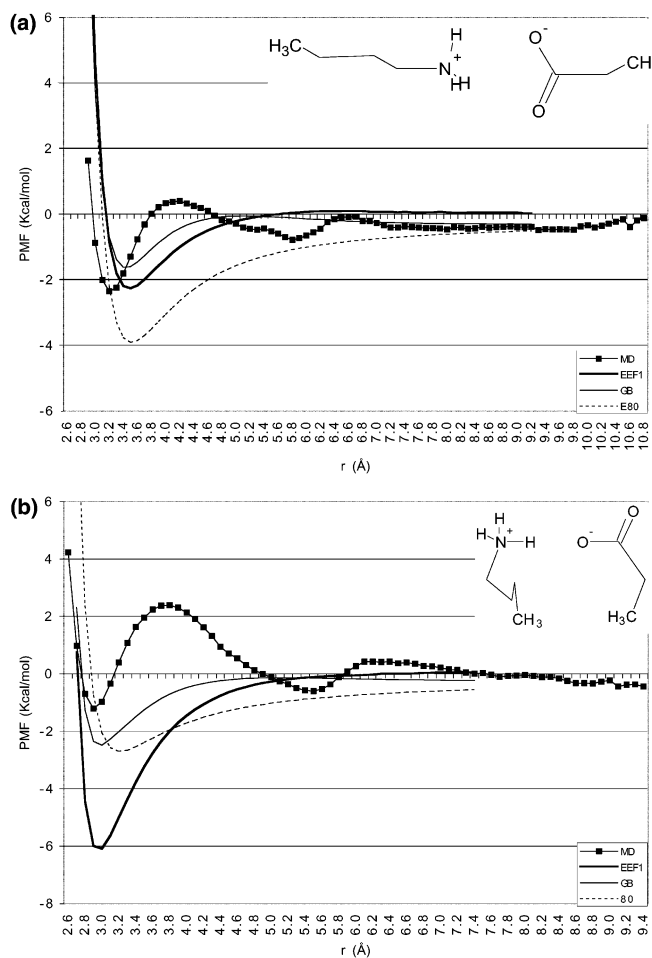


Figure 4. PMF and effective energy curves for the $\text{Lys}^+\dots\text{Glu}^-$ ion pair. (a) collinear approach. r is the distance between the NZ of Lys and the CD of Glu. (b) side-to-side approach. r is the distance between the NZ of Lys and the OE of Glu.

CG atoms of Glu are constrained to be on the same line. In the second (sideways) orientation, the NZ, HZ1 atoms of Lys and CD, OE1 atoms of Glu are constrained to be on a line; the CD, NZ, HZ1 atoms of Lys and the carboxyl are constrained to be on the same plane. The CM is $w = -2.4$ kcal/mol in the head-to-head orientation and -1.2 kcal/mol in the sideways orientation. EEF1 overestimates the CM in the linear H-bonding orientation, but closely matches it in the head-to-head orientation. GB is within 1 kcal/mol from the correct value in both orientations. The uniform dielectric $\epsilon = 80$ overestimates the CM in both orientations.

The PMFs for the $\text{His}\dots\text{Glu}^-$ pair in a linear H-bonding orientation are shown in Figure 5a for protonated His and in Figure 5b for neutral His. Here the two molecules are kept on the same plane and the atoms CD, OE2 of Glu and ND1, HD1 and the center of the CD-NE bond of His are constrained on a line. It is interesting that the CM is deeper for the neutral histidine (-2.5 vs -1.2 kcal/mol). Both $\epsilon = 80$ and GB overestimate the CM for His^+ (no EEF1 model is available for protonated histidine). The CM for neutral His is overestimated by EEF1, underestimated by GB, and matched by $\epsilon = 80$.

The remaining results deal with like-charged ions. In this case, the most probable orientation is less obvious. Dimerization of planar molecules often occurs in one of two orientations: stacked and orthogonal. Although orthogonal structures may be

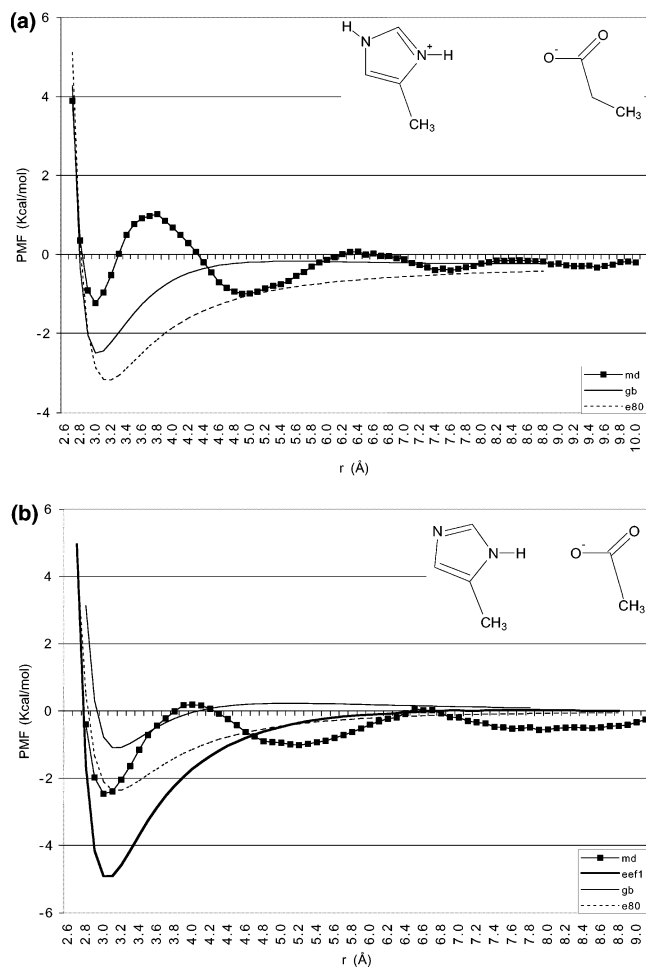


Figure 5. PMF and effective energy curves for the His...Glu⁻ ion pair. r is the distance between the ND1 of His and the OE of Glu. (a) doubly protonated His (b) singly protonated His.

more stable in a nonpolar environment,³⁴ stacking was reported to be preferred in PMF calculations of two guanidinium ions³⁴ and the neutral pair Trp...His in aqueous solution.⁶³ In this work, we consider three possible orientations: stacked, orthogonal, and coplanar.

The results for two Arg⁺ side chains are shown in Figure 6a,b,c. In Figure 6a, the two ions approach in a stacked, antiparallel (staggered) orientation. This arrangement is often observed in crystal structures.^{34,64} The distance between two molecules is allowed to vary but the orientation remains fixed (in contrast to previous work^{33,34}). We find a shallow CM of less than 1 kcal/mol and a slightly deeper SSM. The CM found here is weaker than those previously reported for two guanidinium ions, which ranged from -10 kcal/mol to -2.7 kcal/mol, depending on the water model.^{33,34} GB comes closest to the MD results, whereas $\epsilon = 80$ is too attractive and EEF1 too repulsive.

An alternative coplanar approach of two Arg⁺ ions (Figure 6b) has a CM of about the same energy as infinite separation and a 3.5 kcal/mol barrier for escape from it. Naturally, none of the continuum models reproduce this local minimum. However, a smoothing or coarse-graining of the MD results

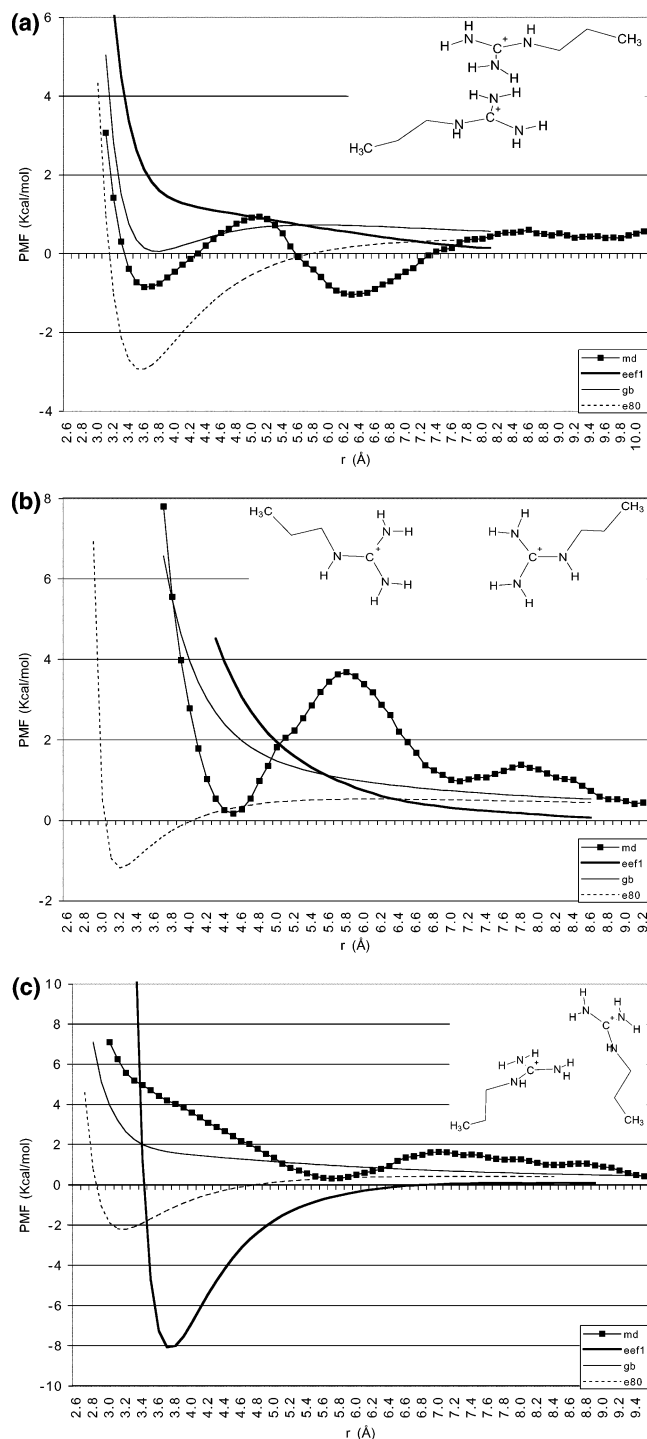


Figure 6. PMF and effective energy curves for the Arg⁺...Arg⁺ ion pair. (a) stacking approach. r is the distance between the CZ atoms. (b) collinear approach. r is the distance between the NH atoms. (c) orthogonal approach. r is the distance between the NH atoms.

would produce curves similar to those of EEF1 and GB; this interaction is essentially repulsive. The primitive model is grossly in error because it is dominated by attractive van der Waals interactions.

Orthogonal approach of two Arg is shown in Figure 6c. Here, the two guanidinium moieties are perpendicular to each other with the HH atoms of one interacting with the NH atoms of the other. This approach produces only a shallow local minimum at about 5.7 Å. As reported previously⁵² EEF1 erroneously

(63) Gervasio, F. L.; Chelli, R.; Marchi, M.; Procacci, P.; Schettino, V. *J. Phys. Chem. B* **2001**, *105*, 7835.

(64) Magalhaes, A.; Maigret, B.; Hoflack, J.; Gomes, J. N. F.; Scheraga, H. A. *J. Protein Chem.* **1994**, *13*, 195.

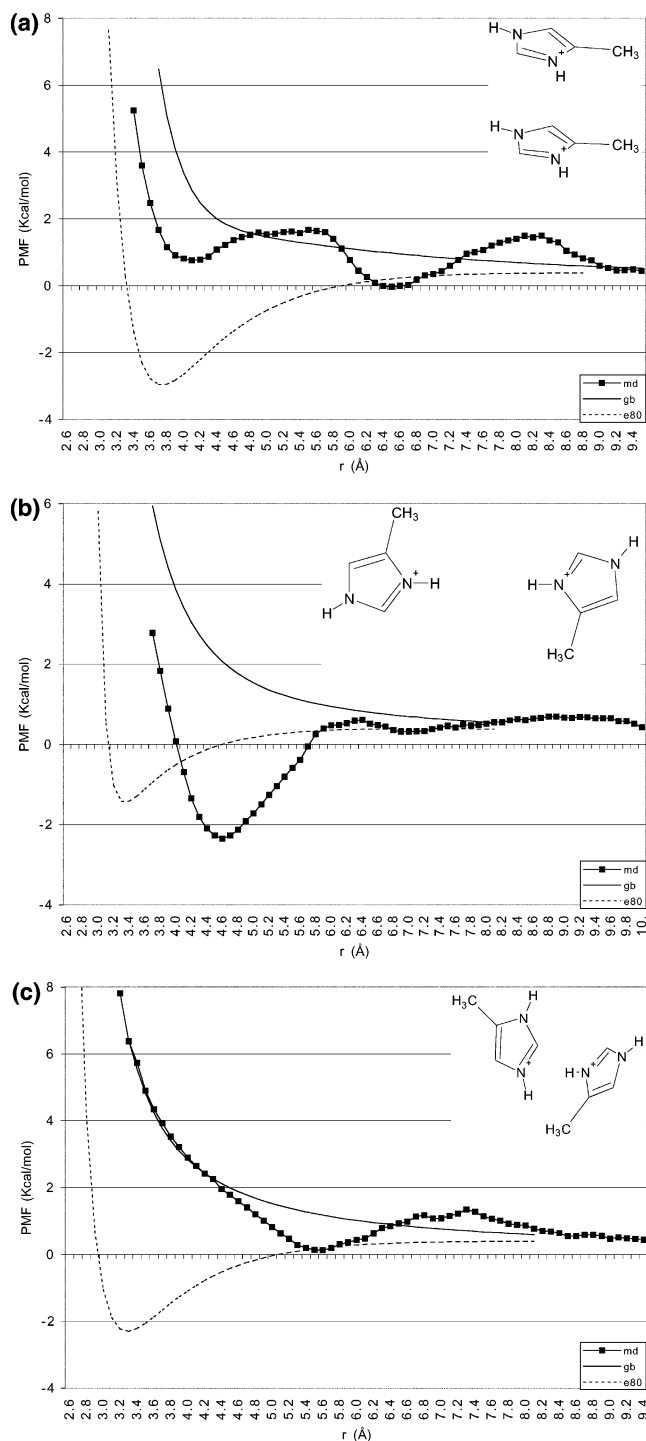


Figure 7. PMF and effective energy curves for the His⁺...His⁺ ion pair. (a) stacking approach. r is the distance between the centers of mass of the two rings. (b) collinear approach. r is the distance between the two N atoms. (c) orthogonal approach. r is the distance between the two N atoms.

predicts a favorable interaction in this orientation, whereas GB is repulsive and not far from the MD results. Again, the primitive model is too attractive with a CM at very short distances.

We also considered 3 different orientations for the pair His⁺...His⁺. In the stacking approach (Figure 7a) the center of mass of the two rings is constrained on a line and the orientation of the two rings is kept the same (parallel). This approach produces two shallow local minima of about 0.8 kcal/mol (CM) and 0 kcal/mol (SSM). Again, the GB model goes through the

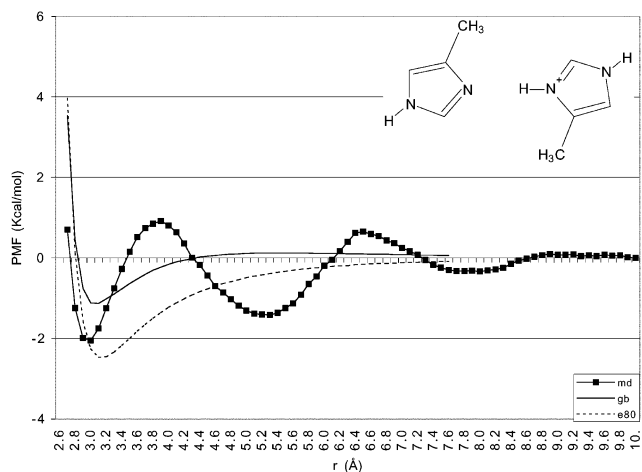


Figure 8. PMF and effective energy curves for the His⁰...His⁺ ion pair. r is the distance between the two N atoms.

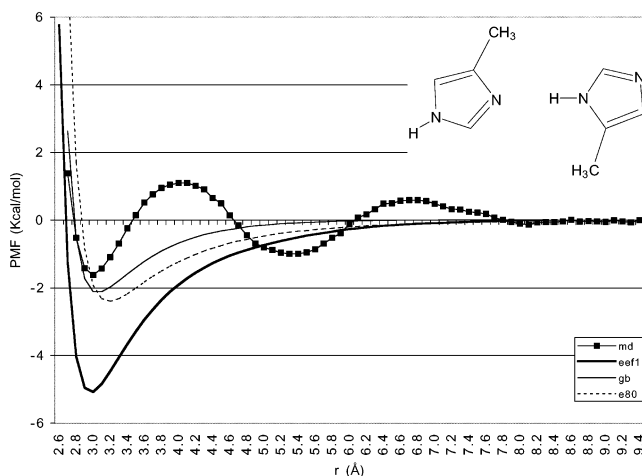


Figure 9. PMF and effective energy curves for the His⁰...His⁰ ion pair. r is the distance between the two N atoms.

MD results, although it rises too fast at short distances. The coplanar approach (Figure 7b) has a stable CM of about -2 kcal/mol and lacks a SSM. GB does not reproduce this stable CM. In the orthogonal approach (Figure 7c), the two rings are perpendicular to each other and the ND1, HD1 atoms of one ring approach the NE2 atom of the other ring. Here, only a shallow SSM is observed, with GB capturing correctly the overall repulsive interaction. Figures 8 and 9 show the results for the linear approach when one or both His are neutral. These two PMFs are similar to each other but differ from the PMF of two protonated His (Figure 7b). Neutralization of at least one His is necessary for close contact and a SSM. For the neutral pair EEF1 overestimates the CM, whereas GB either slightly underestimates or slightly overestimates it. Here, the primitive model is a pretty good approximation.

The PMF for the Arg⁺...His⁺ pair in three orientations is shown in Figure 10a,b,c. In the stacking orientation the CM is unstable and the SSM slightly stable. Coplanar approach produces a slightly stable CM and orthogonal approach produces an unstable SSM. The GB curves are monotonically repulsive but not far from the MD data, and $\epsilon = 80$ predicts large, stable contact minima.

The PMF for the H-bond between Lys⁺ and neutral His (Figure 11) has a repulsive CM of $w = +0.8$ kcal/mol and a

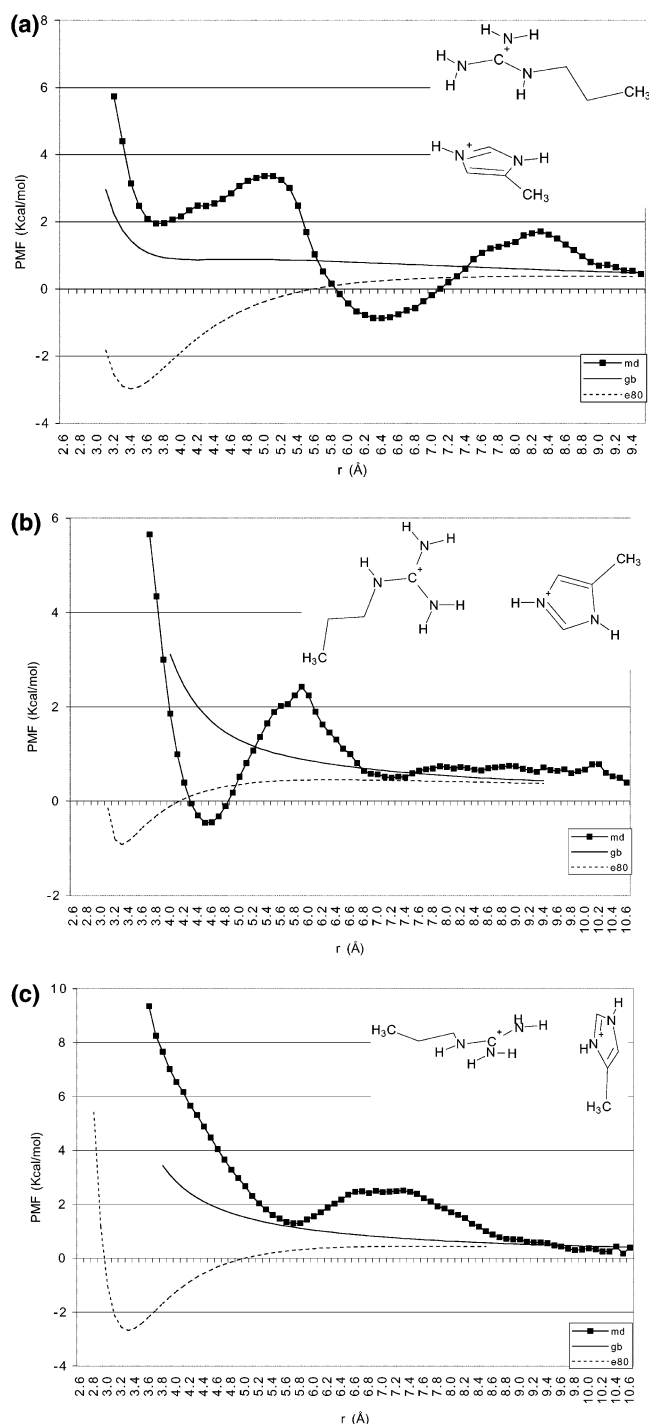


Figure 10. PMF and effective energy curves for the Arg⁺...His⁺ ion pair. (a) stacked orientation. r is the distance between the CZ of Arg and the center of mass of the His ring. (b) collinear approach. r is the distance between the two N atoms. (c) orthogonal orientation. r is the distance between the two N atoms.

solvent-separated minimum of $w = 0.4$ kcal/mol. Both EEF1 and $\epsilon = 80$ predict the contact pair to be stable, whereas GB predicts a monotonic repulsion that rises too fast at short distance. The pair Lys⁺...His⁺ in both linear (Figure 12a) and orthogonal (Figure 12b) approach has only one shallow unstable minimum closely approximated by GB.

The Glu⁻...Glu⁻ pair in a head to head approach (Figure 13a) has a broad and marginally stable CM around 3.8 Å. The depth of the minimum is best predicted by EEF1, whereas GB is too

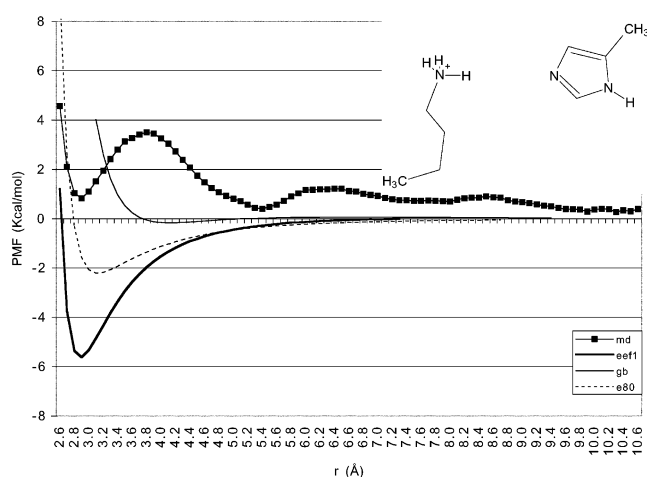


Figure 11. PMF and effective energy curves for the Lys⁺...His⁰ ion pair in collinear approach. r is the distance between the two N atoms.

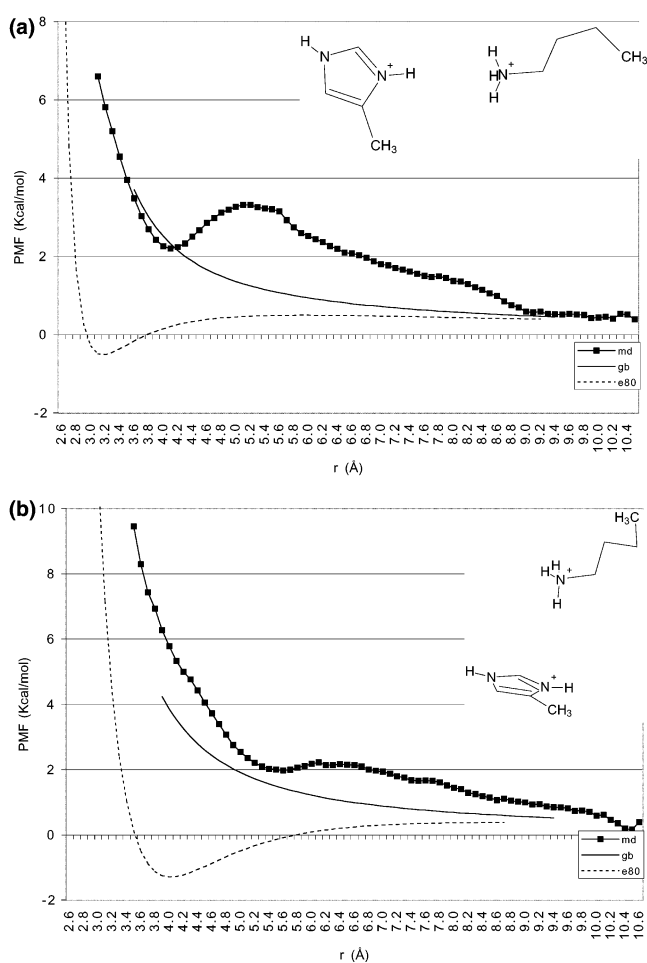


Figure 12. PMF and effective energy curves for the Lys⁺...His⁺ ion pair. r is the distance between the two N atoms. (a) collinear approach. (b) orthogonal approach

repulsive and $\epsilon = 80$ too attractive. An orthogonal approach for the same ion pair (Figure 13b) bringing close oppositely charged atoms gives a very flat PMF. EEF1 and $\epsilon = 80$ are too attractive while GB is too repulsive. The PMFs for H-bonded pairs Glu⁰...Glu⁰ (Figure 14) and Glu⁰...Glu⁻ (Figure 15) are very similar with a contact minimum of about -2 which is best described by $\epsilon = 80$. EEF1 is too attractive for the Glu⁰...Glu⁰

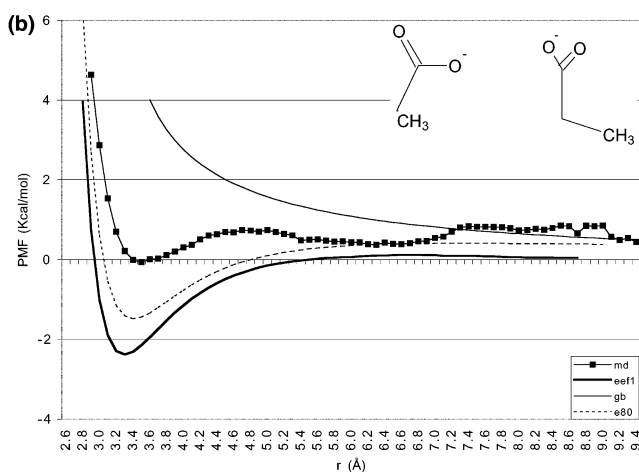
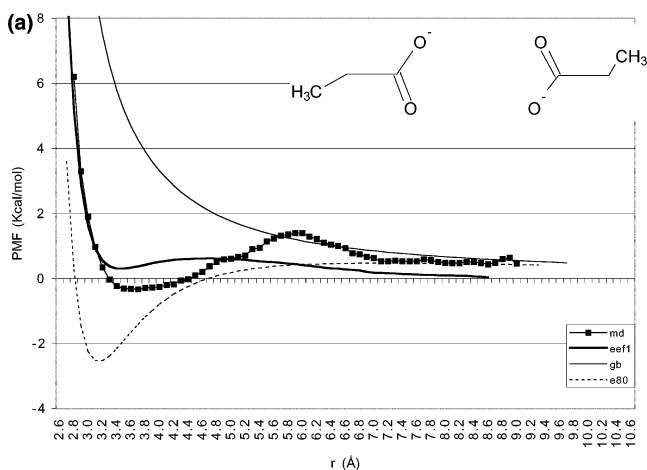


Figure 13. PMF and effective energy curves for the $\text{Glu}^- \dots \text{Glu}^-$ ion pair. (a) collinear approach. r is the distance between the O atoms. (b) orthogonal approach. r is the distance between OE and CD.

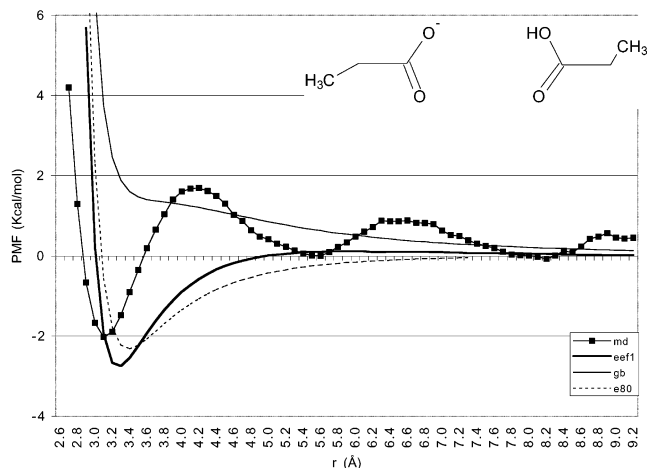


Figure 14. PMF and effective energy curves for the $\text{Glu}^- \dots \text{Glu}^0$ ion pair. r is the distance between the O atoms.

pair but a good approximation for the $\text{Glu}^0 \dots \text{Glu}^-$ pair. GB is too repulsive for both.

The PMF for like-charged ion pair $\text{Lys}^+ \dots \text{Lys}^+$ (Figure 16) has a shallow SSM at 5.2 Å, whereas GB and EEF1 are monotonically repulsive. Local minima at 5–8 Å have been observed for sideways orientation in Lys containing peptides.^{65,66} A similar situation is observed for planar approach of Lys^+ to Arg^+ (Figure 17a). Apart from an unstable, shallow minimum

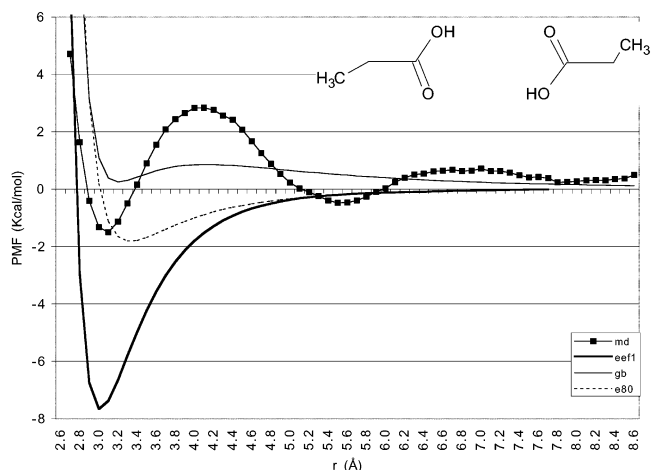


Figure 15. PMF and effective energy curves for the $\text{Glu}^0 \dots \text{Glu}^0$ ion pair. r is the distance between the O atoms.

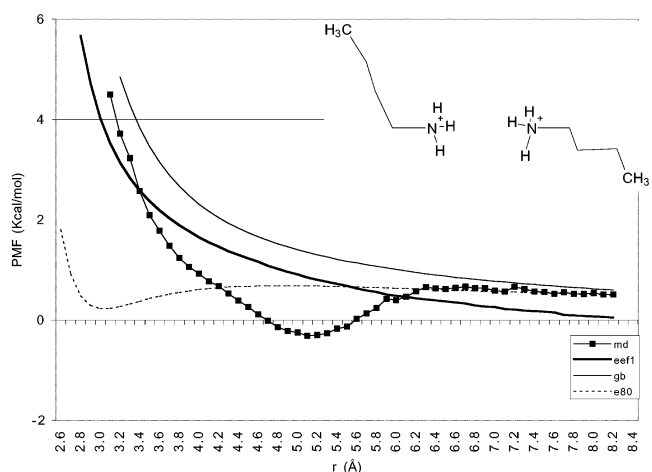


Figure 16. PMF and effective energy curves for the $\text{Lys}^+ \dots \text{Lys}^+$ ion pair. r is the distance between the NZ atoms.

and a barrier, the PMF is captured by the monotonically repulsive curves predicted by EEF1 and GB. The PMF for out of plane approach in the same system (Figure 17b) has a slightly stable minimum. EEF1 and $\epsilon = 80$ match its depth but not its location, whereas GB is too repulsive.

Conclusions

The SSBP boundary potential⁵⁰ gives for monatomic ions results that are physically reasonable and comparable to those obtained by other methods, at very low computational cost. Therefore, it seems a reasonable approach for calculating PMFs in biomolecular systems. In this work, it has been applied to obtain PMFs between charged amino acid side chains at given orientations. The strongest interaction was found for the coaxial, double H-bond forming $\text{Arg}^+ \dots \text{Glu}^-$ approach. The contact minima of the PMFs obtained may serve as lower bounds for the free energy of completely exposed salt bridge formation. We also found a remarkable lack of repulsion between like charged side chains. Indeed, a slight attraction was observed in some cases. This counterintuitive result depends on the balance between Coulomb and solvation effects and was first observed

(65) Vila, J. A.; Ripoll, D. R.; Villegas, M. E.; Vorobjev, Y. N.; Scheraga, H. A. *Biophys. J.* **1998**, *75*, 2637.

(66) Villarreal, M.; Montich, G. *Protein Sci.* **2002**, *11*, 2001.

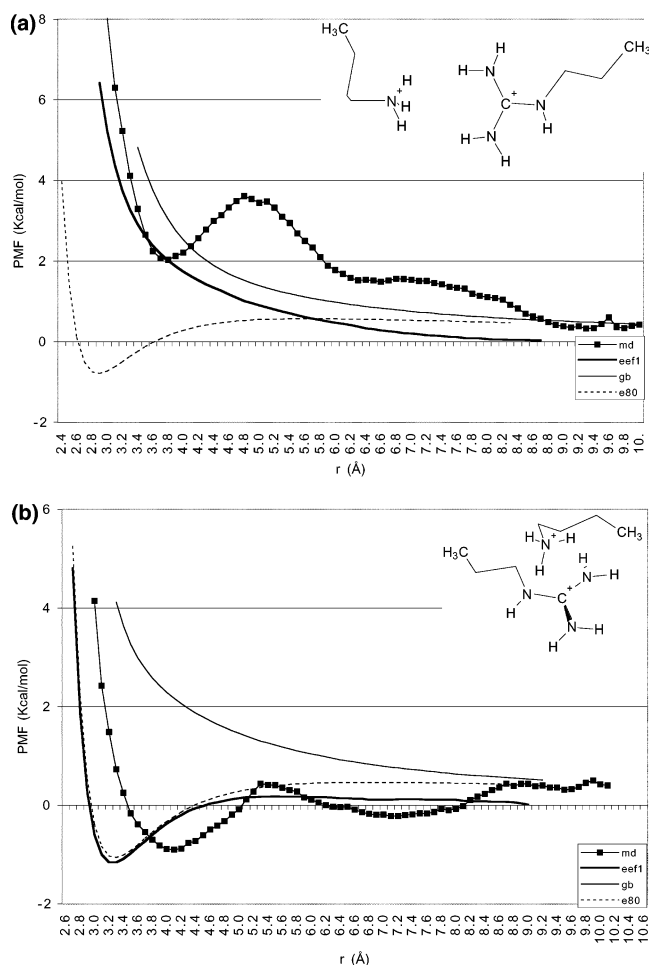


Figure 17. PMF and effective energy curves for the Lys⁺...Arg⁺ ion pair. (a) collinear approach. r is the distance between NZ of Lys and the midpoint of the NH–NH vector in Arg. (b) orthogonal approach. r is the distance between NZ of Lys and CZ of Arg.

in the Cl–Cl system for certain interaction potentials.²⁰ Nevertheless, the attractions are weak.

The performance of the implicit solvation models considered in this work is summarized in Table 1. All continuum models predict only contact minima (if any) for all the salt bridges and H-bonded pairs. The inability of these models to reproduce the oscillations in the PMF is understandably due to their neglect of the discrete nature of the solvent. Whether this deficiency is critical is an open question. It is more likely to affect the kinetics, rather than the thermodynamics of association.⁴² The uniform dielectric model ($\epsilon = 80$) is dominated by van der Waals interactions and predicts all pairs to be stable, either correctly

Table 1. Performance of the Three Implicit Solvation Models with Regard to the Depth of the Contact Minimum

Ion pair	EEF1	GB	$\epsilon = 80$
Glu ⁻ ... Arg ⁺ (head)	A	✓	✓
Glu ⁻ ... Lys ⁺ (head)	✓	✓	A
Glu ⁻ ... Lys ⁺ (side)	A	a	a
Glu ⁻ ... His ⁺ (head)	A	A	A
Glu ⁻ ... His ⁺ (head)	A	r	✓
Arg ⁺ ... Arg ⁺ (stack)	R	✓	A
Arg ⁺ ... Arg ⁺ (head)	✓	✓	A
Arg ⁺ ... Arg ⁺ (orth)	AA	✓	A
His ⁺ ... His ⁺ (stack)		✓	A
His ⁺ ... His ⁺ (head)		R	A
His ⁺ ... His ⁺ (orth)		✓	A
His ⁺ ... His ⁺ (head)		✓	✓
His ... His(head)	A	✓	✓
Arg ⁺ ... His ⁺ (stack)		✓	✓
Arg ⁺ ... His ⁺ (head)		✓	A
Arg ⁺ ... His ⁺ (orth)		✓	A
His ... Lys ⁺ (head)	AA	✓	A
His ⁺ ... Lys ⁺ (head)		✓	A
His ⁺ ... Lys ⁺ (stack)		✓	A
Glu ⁻ ... Glu ⁻ (head)	✓	R	A
Glu ⁻ ... Glu ⁻ (orth)	A	R	✓
Glu ⁻ ... Glu ⁰ (head)	✓	R	A
Glu ⁰ ... Glu ⁰ (head)	A	✓, r	✓
Lys ⁺ ... Lys ⁺ (head)	✓	✓	A
Arg ⁺ ... Lys ⁺ (head)	✓	✓	A
Arg ⁺ ... Lys ⁺ (orth)	✓	R	✓

✓: good, A: too attractive, R: too repulsive, a: somewhat attractive, r: somewhat repulsive, AA: much too attractive.

(and sometimes fortuitously close to the simulation result), or incorrectly (for some like charged pairs which are repulsive at any distance). The model that comes closest to the simulation results is the GB model. However, in some cases it predicts the CM to be weak, or no minimum at all (the most striking example is Glu⁰...Glu⁻). The EEF1 model overestimates the CM in many cases of unlike charged pairs, neutral H-bonds, and especially for out-of plane approach of some like-charged pairs. This deficiency of EEF1 could perhaps be rectified by reducing the polarity of the pseudoionic side chains. A study of the PMFs between two or three methane molecules showed that EEF1 reproduces the contact minima quite well.⁴²

It is hoped that the results obtained here can be used as a benchmark for parametrization and testing of implicit solvation models. An Excel file with all numerical results are available from the authors upon request.

Acknowledgment. We thank C.L. Brooks and M.S. Lee for sharing their WHAM program. This work was supported by the National Science Foundation (DBI-9974621).

JA025521W